

Combustion for aerospace propulsion

# Stabilization of non-premixed flames in supersonic reactive flows

Jean-Francois Izard \*, Arnaud Mura

LCD UPR9028 CNRS, ENSMA, 1, avenue Clément-Ader, BP 40109, 86961 Futuroscope Chasseneuil, France

Available online 21 July 2009

## Abstract

A Lagrangian framework is set out to describe turbulent non-premixed combustion in high speed coflowing jet flows. The final aim is to provide a robust computational methodology to simulate, in various conditions, the underexpanded GH<sub>2</sub>/GO<sub>2</sub> torch that is used to initiate combustion in an expander cycle engine. The proposed approach relies on an early modelling proposal of Borghi and his coworkers. The model is well suited to describe finite rate chemistry effects and its recent extension to high speed flows allows one to take the influence of viscous dissipation phenomena into account. Indeed, since the chemical source terms are highly temperature sensitive, the influence of viscous phenomena on the thermal runaway is likely to be all the more pronounced since the Mach number values are high. The validation of the extended model has been recently performed through the numerical simulation of two distinct well-documented experimental databases. Only a brief summary of this preliminary validation step is provided here. The main purpose of the present work is to proceed with the numerical simulation of geometries that bring together the essential peculiarities of the underexpanded GH<sub>2</sub>/GO<sub>2</sub> torch. The behavior of the corresponding supersonic coflowing jet flames for various conditions is discussed in the light of computational results. *To cite this article: J.-F. Izard, A. Mura, C. R. Mecanique 337 (2009).*

© 2009 Académie des sciences. Published by Elsevier Masson SAS. All rights reserved.

## Résumé

**Stabilisation des flammes non prémélangées dans les écoulements supersoniques réactifs.** Une approche Lagrangienne est introduite pour décrire les flammes turbulentes non prémélangées dans des jets co-courants supersoniques. L'objectif final est de disposer d'un modèle numérique robuste pour la simulation de la torche sous-détendue GH<sub>2</sub>/GO<sub>2</sub> utilisée comme système d'allumage dans un moteur fusée. L'approche retenue repose sur les travaux de Borghi et de ses collaborateurs. Elle permet de décrire les effets de chimie finie et sa récente extension aux écoulements à grandes vitesses permet de prendre en compte l'influence des phénomènes liés à la dissipation visqueuse. En effet, les termes sources chimiques étant fortement sensibles à la température, l'influence des phénomènes visqueux sur l'emballlement thermique devient d'autant plus importante que le nombre de Mach est grand. La validation du modèle étendu a été récemment effectuée en considérant deux cas expérimentaux de référence. Cette étape préliminaire de validation est brièvement résumée mais le but essentiel de la présente étude est de procéder maintenant à la simulation numérique de configurations regroupant les particularités de la torche sous-détendue GH<sub>2</sub>/GO<sub>2</sub>. Le comportement des flammes jet supersoniques correspondant aux différentes conditions est discuté à la lumière des résultats des simulations numériques. *Pour citer cet article : J.-F. Izard, A. Mura, C. R. Mecanique 337 (2009).*

© 2009 Académie des sciences. Published by Elsevier Masson SAS. All rights reserved.

**Keywords:** Combustion; Lagrangian modelling; Supersonic combustion; Viscous effects; Underexpanded jets

\* Corresponding author.

E-mail addresses: [jean-francois.izard@lcd.ensma.fr](mailto:jean-francois.izard@lcd.ensma.fr) (J.-F. Izard), [arnaud.mura@lcd.ensma.fr](mailto:arnaud.mura@lcd.ensma.fr) (A. Mura).

Mots-clés : Combustion ; Modèle Lagrangien ; Combustion supersonique ; Effets visqueux ; Jets sous-détendus

## 1. Introduction

In rocket engine applications, ignition phenomena, as well as eventual re-ignition in space, are of primary concern. However, their experimental investigation in rocket engine conditions still remains difficult and often incomplete; accordingly, reliable and robust numerical tools are still needed to perform design and parameter studies of such reactive flow configurations. In the specific case of a GH<sub>2</sub>/GO<sub>2</sub> torch igniter, the peculiar flow configuration gives birth to a Mach disk featuring triple point conditions, the stability of which being still an open question even in non-reactive situations. The turbulent non-premixed flame that is expected to stabilize within the mixing layers, where favorable conditions are reached, needs to be studied in detail and the phenomena that drive the associated stabilization process must be taken into account in the final modelling proposal. Lagrangian strategies have been previously retained for their robustness and affordable computational costs to describe turbulent mixing and combustion either in supersonic coflowing jets [1] or in a laboratory scramjet geometry [2]. However, these previous studies did not address the modelling of the ignition phenomena associated with the conversion of kinetic energy into thermal energy via the viscous dissipation heating, a mechanism that is likely to affect the early developments of the chemical processes in high Mach number reactive flows. Even if the corresponding phenomena do not bring special additional difficulties to the simulation of laminar reactive flows, the situation is different from the turbulent combustion modelling point of view and some efforts have been already done to take them into account under the fast chemistry assumption. For instance, a revisited flamelet model has been put forward for non-premixed combustion in supersonic reactive flows by Sabel'nikov et al. [3]. Nevertheless, this issue remains challenging for situations where finite rate chemistry effects come into play. A possible way to include such an influence for high velocity reactive flows is described below within the MIL framework of turbulent non-premixed combustion. The reliability of this proposal has been recently assessed for gaseous conditions through the numerical simulation of two well-documented experimental databases and it is carried out herein with the investigation of the central GH<sub>2</sub>/GO<sub>2</sub> igniter.

The present manuscript is organized as follows: the essential characteristics of the model are briefly recalled in the next section. It is followed by a synthetic description of the retained numerical methodology. Results of numerical simulations are then reported for: (i) supersonic reactive coflowing jets at atmospheric pressure; and (ii) highly under-expanded supersonic coflowing jets. Finally, the article ends with a brief section where conclusions are drawn from the numerical simulations and future works are presented.

## 2. The Lagrangian intermittent model

The MIL (Modèle Intermittent Lagrangien) representation of turbulent non-premixed combustion essentially describes the competition that takes place between micro-mixing phenomena and finite rate chemistry effects. The main features of this model, introduced in the early works of Borghi and Gonzalez [4], are briefly recalled below.

### 2.1. Joint scalar PDF estimation

The MIL model is a Lagrangian model in the composition space which is based on the knowledge of two scalar variables, namely the mixture fraction  $\xi$  and the mass fraction of a reactive species  $Y$  which indicates the progress of the chemical reaction. The oxygen mass fraction has been retained as  $Y$  in the present study. The MIL model relies on the sudden chemistry assumption [4], thus permitting a strong but clearly stated functional dependence between the two scalars to be introduced:  $Y = Y^{\text{MIL}}(\xi)$ . As a result, the estimation of the joint scalar Probability Density Function (PDF)  $\tilde{P}(Y, \xi; \mathbf{x}, t)$  can be simply expressed from the knowledge of the marginal mixture fraction PDF  $\tilde{P}(\xi; \mathbf{x}, t)$ . If the latter is represented thanks to the usual Beta function PDF, the joint scalar PDF can be written  $\tilde{P}(Y, \xi; \mathbf{x}, t) = \beta(\tilde{\xi}, \tilde{\xi}''^2)P(Y | \xi; \mathbf{x}, t)$  where the conditional PDF is closed by considering the MIL trajectory:  $P(Y | \xi; \mathbf{x}, t) = \delta(Y - Y^{\text{MIL}}(\xi))$ .

The presumed Beta shape is fully determined provided that both mean  $\tilde{\xi}$  and variance  $\tilde{\xi}''^2$  of the mixture fraction are known. These quantities are calculated through the numerical resolution of the following set of transport equations:

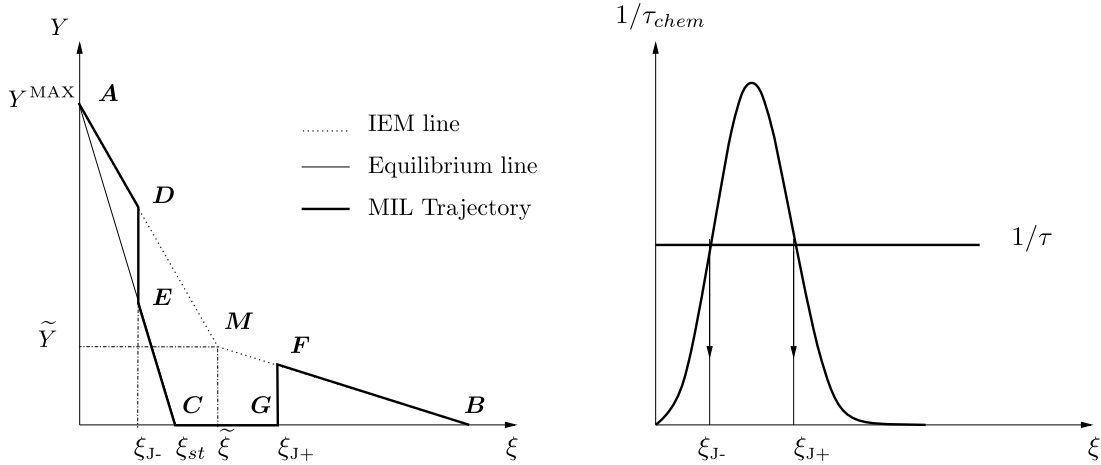


Fig. 1. Representation of the MIL trajectory (thick lines) in the plane  $(\xi, Y)$ . Equilibrium (plain line) and IEM mixing lines (dashed lines) are also depicted. Ignition domain  $[\xi_{J-}; \xi_{J+}]$  as obtained by a direct comparison between  $\tau$  and  $\tau_{chem}$ .

$$\frac{\partial \bar{\rho} \tilde{\xi}}{\partial t} = -\frac{\partial}{\partial x_k} \left( \bar{\rho} \tilde{u}_k \tilde{\xi} - \bar{\rho} \frac{v_T}{Sc_{\tilde{\xi}}} \frac{\partial \tilde{\xi}}{\partial x_k} \right); \quad \frac{\partial \bar{\rho} \tilde{\xi}''^2}{\partial t} = -\frac{\partial}{\partial x_k} \left( \bar{\rho} \tilde{u}_k \tilde{\xi}''^2 - \bar{\rho} \frac{v_T}{Sc_{\tilde{\xi}''^2}} \frac{\partial \tilde{\xi}''^2}{\partial x_k} \right) + 2\bar{\rho} \frac{v_T}{Sc_{\tilde{\xi}}} \frac{\partial \tilde{\xi}}{\partial x_k} \frac{\partial \tilde{\xi}}{\partial x_k} - \bar{\rho} \frac{\tilde{\xi}''^2}{\tau_{\xi}}$$

where laminar diffusion terms are neglected with respect to their turbulent counter parts. The corresponding turbulent scalar transport terms are closed by using the turbulent eddy viscosity  $v_T = C_{\mu} k^2 / \epsilon$ , with  $C_{\mu} = 0.09$ , and the turbulent Schmidt numbers  $Sc_{\tilde{\xi}}$  and  $Sc_{\tilde{\xi}''^2}$  are set to their usual value of 0.7. The mean dissipation rate of the scalar variance is modelled with a standard linear relaxation law using the dissipation time scale  $\tau_{\xi}$  discussed later. It is noteworthy that since the MIL skeleton is made up of linear relationships between  $Y$  and  $\xi$ , see Fig. 1, all the integral terms that appear through the weighting by the mixture fraction PDF  $\tilde{P}(\xi)$  can be expressed directly using the standard algorithms from the Numerical Recipes Library [5].

## 2.2. Lagrangian path in the composition space

Scalar micro-mixing terms are represented with the classical IEM model [6] leading to the following two Lagrangian equations for the mixture fraction  $\xi$  and the reactive variable  $Y$  [7]:

$$\frac{d\xi}{dt} = \frac{1}{\bar{\rho}} \left\langle \frac{\partial}{\partial x_k} \left( \rho D \frac{\partial \xi}{\partial x_k} \right) \middle| \xi \right\rangle = \frac{\tilde{\xi} - \xi}{\tau_{\xi}}; \quad \frac{dY}{dt} = \frac{1}{\bar{\rho}} \left\langle \frac{\partial}{\partial x_k} \left( \rho D \frac{\partial \xi}{\partial x_k} \right) \middle| \xi \right\rangle + \langle \omega_Y | \xi \rangle = \frac{\tilde{Y} - Y}{\tau_Y} + \omega_Y \quad (1)$$

where  $\tau_{\xi}$  and  $\tau_Y$  are the characteristic mixing time scales of the mixture fraction and the oxygen mass fraction respectively. These quantities can be evaluated either thanks to an algebraic relationship based on the integral turbulent time scale  $\tau_T = k/\epsilon$ , or through the resolution of a transport equation for the mean scalar dissipation rate. Nevertheless, it should be recognized that the closure of such a transport equation for a reactive scalar still suffers from certain uncertainties and further work is also needed in this direction [8,9].

Within the MIL framework, it is assumed that the chemical reactions are sudden: particles need a finite time to ignite during their evolution towards the mean composition but then instantaneously jump from the mixing line to the equilibrium line. Their trajectory can be drawn in the composition space for fixed values of mean composition and mixing frequency, as sketched in Fig. 1.

A more detailed inspection of the system of Eqs. (1) for  $\xi$  and  $Y$  leads to different responses depending on the values of the characteristic mixing time scales  $\tau_{\xi}$  and  $\tau_Y$ . On the IEM mixing lines, the chemical source terms can be neglected with respect to the mixing terms and the system (1) becomes:

$$dY/d\xi = (\tilde{Y} - Y)/(\tilde{\xi} - \xi) \quad (2)$$

where it has been supposed that  $\tau_{\xi} = \tau_Y = \tau$ . This hypothesis is not restrictive since, before combustion occurs, the differences between  $\tau_{\xi}$  and  $\tau_Y$  are expected to be small enough. Here,  $\tau = C_{\xi} \cdot \tau_T$  with  $C_{\xi}$  a modelling constant set

equal to 0.5. The previous equation (2) can be integrated to give the branches AM and BM of Fig. 1. On the equilibrium trajectory, either  $Y = 0$  on the branch corresponding to rich mixtures, or  $Y = Y^{\text{MAX}}(\xi_{st} - \xi)/\xi_{st}$  on the branch of lean mixtures, where  $\xi_{st}$  is the stoichiometric mixture fraction value. This corresponds to the segments BC and AC in Fig. 1. Finally, the MIL trajectory is fully determined through the knowledge of the jump positions  $\xi_{j-}$  and  $\xi_{j+}$ . Following the methodology described in [7], these positions are easily obtained by a direct comparison between the mixing time scale  $\tau$  and the tabulated chemical time scales, see Fig. 1. In the present study, the latter have been obtained using the detailed mechanism proposed by Jachimowski [10] that includes 13 species and 33 elementary chemical reaction steps. Thanks to the consideration of the Lagrangian trajectory  $Y^{\text{MIL}}(\xi)$ , the MIL approach provides a higher probability for fluid particles to burn at nearly stoichiometric compositions. Moreover, a wide range of combustion regimes can be handled, from the infinitively fast chemistry to complete extinction.

### 2.3. Evaluation of the chemical production rate

The resulting Lagrangian path approximated with broken lines provides the MIL trajectory, see Fig. 1. On such a trajectory, the instantaneous production rate of  $Y$  is given by:

$$\omega_Y = 1/\tau [(dY/d\xi)(\tilde{\xi} - \xi) - (\tilde{Y} - Y)] \tag{3}$$

- On the segments AD and BF, fluid particles follow the IEM mixing trajectory with no significant reaction. This is recovered by inserting Eq. (2) into Eq. (3) which yields  $\omega_Y^{\text{IEM}} = 0$ .
- Then, once ignition has occurred, particles reach instantaneously the fully burned products lines following the paths DE and FG. It can be established that the corresponding contributions to the instantaneous production rate are respectively given by:  $\omega_Y^{\text{J-}} = \delta Y_{\text{J-}}(\tilde{\xi} - \xi_{\text{J-}})/\tau$  for  $\xi_{\text{J-}} < \tilde{\xi}$  and  $\omega_Y^{\text{J+}} = \delta Y_{\text{J+}}(\tilde{\xi} - \xi_{\text{J+}})/\tau$  for  $\xi_{\text{J+}} > \tilde{\xi}$ . In the previous expressions,  $\delta Y_{\text{J-}}$  and  $\delta Y_{\text{J+}}$  denote, respectively, the differences between the IEM and the equilibrium values of  $Y$  at these jump locations, see [7].
- Along the segments EC and GC, fluid particles follow the equilibrium line, and it can be shown that:
  - on the segment EC,  $dY/d\xi = -Y^{\text{MAX}}/\xi_{st}$ , which implies:  $\omega_Y^{\text{EQU}} = -\tilde{Y}\xi_{st} - Y^{\text{MAX}}(\xi_{st} - \tilde{\xi})/\tau\xi_{st}$ ,
  - on the segment GC,  $Y = 0$  and  $dY/d\xi = 0$ , so that:  $\omega_Y^{\text{EQU}} = -\tilde{Y}/\tau$ .

Thus, the instantaneous reaction rate can be expressed as the sum of the following contributions:

$$\omega_Y^{\text{MIL}} = \omega_Y^{\text{IEM}} + \omega_Y^{\text{J-}} + \omega_Y^{\text{J+}} + \omega_Y^{\text{EQU}} \tag{4}$$

The first term in the RHS of this latter equation has been shown to be zero everywhere. The second and third contributions are zero except at the jump locations i.e.  $\xi_{\text{J-}}$  and  $\xi_{\text{J+}}$ . The fourth contribution results from the slope difference that can exist between IEM-LMSE and equilibrium lines. Provided that the MIL trajectory is known, namely that the mean values  $\tilde{\xi}$ ,  $\tilde{Y}$  and the mixing time scale  $\tau$  have been evaluated, the mean chemical rate  $\overline{\rho\omega_Y} = \overline{\rho}\tilde{\omega}_Y^{\text{MIL}}$  is simply obtained by weighting Eq. (4) with the PDF of the mixture fraction. The resulting value is finally used as an input to solve the modelled transport equation for the reactive species  $\tilde{Y}$  [7,11].

### 2.4. Extension to high velocity flows

For high velocity flows, the Lagrangian description requires the consideration of an additional variable which takes into account the influence of the kinetic energy. The total enthalpy  $h_t$  is retained to this purpose. Luo and Bray [12] suggested that conserved scalar presumed PDF methods can be extended to high speed combustion by replacing the static enthalpy with the stagnation enthalpy. The validity of this working hypothesis is strongly related to the existence of a linear algebraic relationship between the mixture fraction and the stagnation enthalpy, a relationship which theoretically holds only if the Lewis and Prandtl numbers are unity and if the effects induced by the temporal variations of pressure remain negligible. Despite these restrictive assumptions, this behavior is rather well supported by DNS studies [12] and accordingly, we write the Lagrangian evolution of the total enthalpy as follows:

$$dh_t/dt = (\tilde{h}_t - h_t)/\tau \tag{5}$$

Therefore, for a geometry fed with two inlets: oxidizer and fuel streams (0) and (1) respectively, the following set of linear relationships holds:  $h_t(\xi) = \tilde{h}_t + (\tilde{h}_t - h_t^0)(\xi - \tilde{\xi})/\tilde{\xi}$  for  $\xi \in [0; \tilde{\xi}]$  and  $h_t(\xi) = \tilde{h}_t + (h_t^1 - \tilde{h}_t)(\xi - \tilde{\xi})/(1 - \tilde{\xi})$

for  $\xi \in [\tilde{\xi}; 1]$ . For a given value of the mixture fraction, the static enthalpy is evaluated through the simplified relationship:  $h(\xi) = h_t(\xi) - \tilde{u}_i \tilde{u}_i / 2$  which is strictly exact as long as the turbulent Mach number  $M_t$  based on the turbulent kinetic energy remains negligible with respect to the Mach number based on the mean velocity. In each control volume of the computational domain, the resulting knowledge of  $h$  together with the local pressure, which is supposed to be uniform and equal to its mean value  $p = \bar{p}$ , allows one to evaluate the value of the ignition time as a function of the mixture fraction only, but with the added functional dependence on velocity through the consideration of the stagnation enthalpy. Finally, the ignition time scale  $\tau_{ig}$  is tabulated as a function of pressure, mixture fraction, and temperature. Then, a direct comparison between this chemical time scale and an estimated *convection* time scale or particle age allows the identification of a self-ignition domain in the composition space. Such a *convection* time scale or particle age  $\tau_a$  is the time needed by a Lagrangian particle to reach a given value of the mixture fraction  $\xi$  from its originating stream of pure oxidizer (0) or pure fuel (1). Its value is obtained by integrating the Lagrangian trajectory along the IEM pathlines as previously proposed by Izard and Mura [11,13]. Hence, the strong coupling between velocity and chemical reaction is represented through the positions of the jumps  $\xi_{j-}^{ig}$  and  $\xi_{j+}^{ig}$  that are determined by the direct comparison between the particle age  $\tau_a$  and the chemical induction time  $\tau_{ig}$ . Such an extension allows for instance to represent self-ignition phenomena that can result from viscous dissipation effects in supersonic mixing layers.

### 2.5. Compressible turbulence modelling

Among the different modelling proposals available to represent the compressible effects on turbulence within the framework of a  $k-\epsilon$  approach, the strategy introduced by Zeman et al. [14] has been retained to take the high Mach number influence into account. In particular, the pressure dilatation term that appears in the turbulent kinetic energy transport equation is closed as a function of  $M_t$ , the turbulent Mach number based on the turbulent kinetic energy

$$\Pi_d \equiv \overline{p' \partial u_i'' / \partial x_i} = -2C_{\Pi_d} \bar{\rho} S_{ij}^* S_{ij}^* k^2 / \epsilon$$

for  $M_t > M_{tc}$ , and  $\Pi_d = 0$  elsewhere. In the previous expression,  $M_{tc} = 0.1\sqrt{(\gamma + 1)/2}$ , with  $\gamma$  the heat capacity ratio and  $S_{ij}^*$  is defined as  $S_{ij}^* = (2S_{ij} - \delta_{ij} \cdot S_{kk}/3)$  with  $S_{ij}$  the strain rate tensor.

In compressible turbulent flows, the dissipation rate of the turbulent kinetic energy consists of two contributions

$$\bar{\rho} \epsilon = \bar{\rho} \epsilon_s + \bar{\rho} \epsilon_c = 2\overline{\mu \omega_{ij}'' \omega_{ij}''} - 4/3 \overline{\mu \partial u_k'' / \partial x_k \cdot \partial u_k'' / \partial x_k}$$

where  $\omega_{ij}''$  represents the fluctuating vorticity. The first term is the classical solenoidal contribution which is considered to be unaffected by compressible effects. A classical modelled transport equation is retained for this term. The second term is associated to the so-called compressible dissipation rate or dilatational dissipation  $\epsilon_c$  and it is modelled as:  $\epsilon_c = 0.75\epsilon_s (1 - \exp(-[(M_t - M_{tc})/\sigma_c]^2))$  where  $\sigma_c = 0.6$  for  $M_t > M_{tc}$ , and  $\epsilon_c = 0$  elsewhere.

## 3. Computational model for supersonic reactive flow simulations

The model discussed in the previous section has been implemented into the Computational Fluid Dynamics (CFD) code *N3S-Natur* [15]. *N3S-Natur*, used by the SAFRAN group and its partners, solves the three-dimensional compressible and reactive Navier–Stokes equations; it is based on a mixed Finite Volume (FV)/Finite Element (FE) approach applied on 2D or 3D unstructured meshes made up of multiple elements. As displayed in Fig. 2 in the case of a 2D computational grid made up of triangular elements, the boundary  $\Gamma_i$  of each surface  $C_i$  is formed by linking the middles of the segments  $M_{ij}$  between the node  $i$  and each neighboring node  $j$  with the centres of gravity  $G_k$  of each neighboring triangle  $\Gamma_k$  sharing this node  $i$ . The numerical integration is splitted into two distinct parts: the convective terms are integrated using a finite volume approximation while the integration of the divergence of the diffusive fluxes is performed by using the finite element approach on each triangle intersecting  $C_i$ .

The use of the MUSCL (Monotone Upstream-centered Schemes for Conservation Laws) method, combined with flux-limiting functions, leads to a TVD (Total Variation Diminishing) numerical scheme yielding second-order spatial accuracy and avoiding the merging of spurious numerical oscillations in the vicinity of discontinuities. This numerical strategy has been found robust enough to compute a large variety of compressible reactive or non-reactive flows [13].

Considering now the discharge of axisymmetrical underexpanded jets, various morphologies are expected, depending on the value of the Nozzle Pressure Ratio (NPR), a key parameter used to classify them. Their complexity

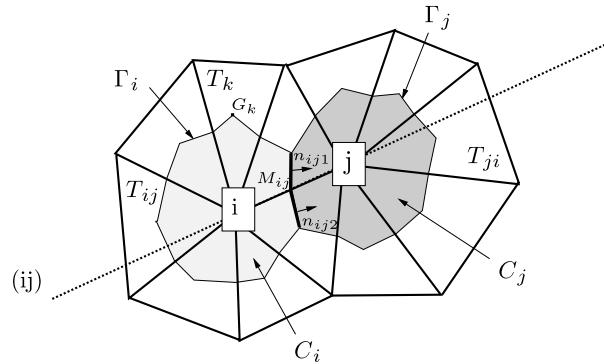


Fig. 2. Representation of the mixed FV/FE discretization method in a bidimensional case.

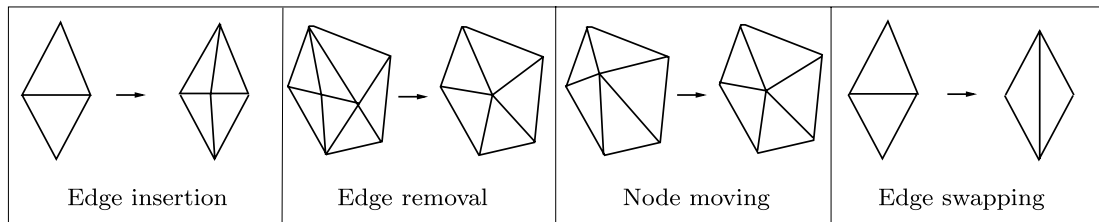


Fig. 3. Local elementary operations used in the AMA algorithm.

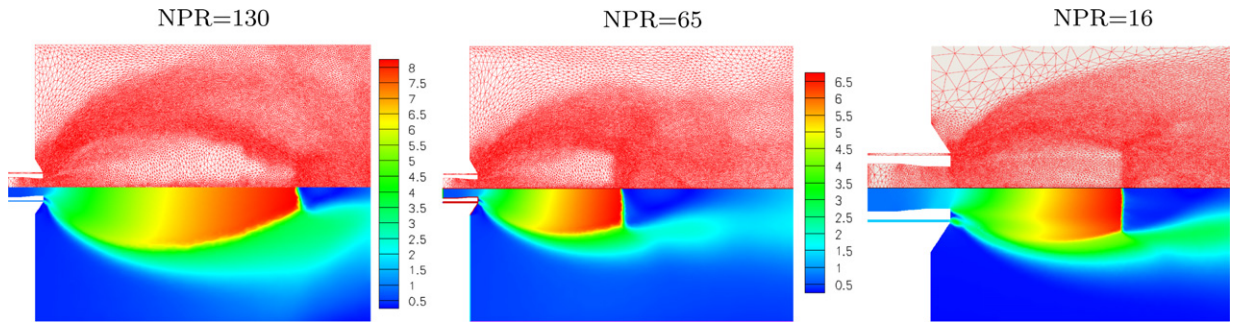


Fig. 4. Computational grids retained to simulate underexpanded jets after application of the mesh adaptation strategy developed by Dolejsi. The lower part of the figures displays the Mach number field.

requires one to resort to a careful mesh adaptation strategy in order to obtain reasonably mesh-independent results. The Anisotropic Mesh Adaptation (AMA) strategy of Dolejsi [16] has then been coupled with the numerical CFD code described above. The AMA method starts from a converged solution obtained by using a linear FE spatial approximation on an initial triangular mesh. Then, it generates an appropriate new metric space in order to evaluate the lengths of the segments, by weighting these as a function of the local curvature level of the appropriate scalar field chosen (the density in the present case). Based on the targeted number of elements for the new mesh, a reference length minimizing the interpolation error is determined. A given set of basic local operations is iteratively applied on the edges to obtain a more isotropic distribution of the interpolation error, see Fig. 3.

In the physical space, this strategy does not only consist in inserting or removing nodes in high gradients or low varying zones respectively, but it also yields a better alignment of the control volumes along the various discontinuities so that the fluxes are more correctly evaluated in the direction of the propagation of the physical waves [17]. Three examples of this mesh adaptation strategy are reported in Fig. 4. This figure clearly demonstrates the ability of the mesh adaptation strategy to realign cells according to the chosen variable field, which can turn to be very efficient to improve the quality of the numerical discretization for the present simulations of highly underexpanded jets.

Table 1  
Boundary conditions used for the simulation of the test case of Cheng et al. [18].

Inlet	Ma	$\tilde{u}$ [m/s]	$\tilde{T}_t$ [K]	$\bar{p}$ [ $10^5$ Pa]	$\tilde{Y}_{O_2}$	$\tilde{Y}_{H_2O}$	$\tilde{Y}_{H_2}$	$\tilde{Y}_{N_2}$
Fuel	1.0	1780	650	1.12	0	0	1.0	0
Air	2.0	1420	2250	1.07	0.245	0.175	0	0.580

#### 4. Supersonic coflowing reactive jets at atmospheric pressure

Several experimental geometries have been designed to perform non-intrusive optical diagnostics in supersonic coflowing jets of hydrogen and vitiated air. Among them, the non-premixed jet flame studied experimentally by Cheng et al. [18] has been first retained as a preliminary test case. It consists of a supersonic burner that provides a choked main jet of hydrogen, used as fuel, surrounded by an annular axisymmetric hot coflowing jet of vitiated air ( $\tilde{Y}_{O_2} = 0.175$ ) at Mach 2. The vitiated air stream is accelerated through a convergent–divergent nozzle and reaches Mach 2 at a temperature of 1250 K; this corresponds to a total temperature  $T_t = 2250$  K, see Table 1. Such a high value of the total temperature is sufficient to promote the stabilization of the diffusion flame through the viscous dissipation mechanism that takes place within the mixing layer and influences the early developments of the chemical processes.

Since both streams are slightly above ambient pressure, a system of successive low amplitude compression and expansion waves is expected. Experimental profiles of average data and associated Root Mean Square (RMS) values have been gathered at seven distinct downstream locations for the major chemical species, namely  $N_2$ ,  $O_2$ ,  $H_2$  and  $H_2O$ , but also for the OH radical and temperature. They have been evaluated from 500 to 2000 independent laser shots [18]. The obtained experimental RMS values confirm that temperature and species fluctuations levels can reach up to 20 and 40%, respectively, which emphasize that neglecting the effects of such fluctuations on the chemical reaction rate can significantly influence the description of the turbulent reactive flow field. The experimental conditions are summarized in Table 1 where  $\tilde{Y}_{O_2}$ ,  $\tilde{Y}_{H_2O}$ ,  $\tilde{Y}_{H_2}$  denote the average mass fraction of chemical species,  $\tilde{u}$  is the axial velocity, Ma the Mach number,  $\tilde{T}_t$  the mean total temperature.

The first interesting qualitative result is that the numerical simulation described below demonstrates that the proposed model is able to represent two expected features associated to the considered coflowing jets flame geometry: (i) the lift-off of the supersonic non-premixed flame; and (ii) the importance of the self-ignition phenomena in the associated mechanism of stabilization. Indeed, the ability of the MIL model to take into account finite-rate chemistry effects and fluctuations of composition enables to recover a lift-off zone in the physical space where both convection and turbulent mixing effects are so important that non-premixed combustion cannot be sustained. The experimental investigations have shown that the first detectable OH molecules can be observed at  $x/D = 10.8$ . The corresponding location is nearly the same as that associated to the first increase in temperature observed in the numerical simulation, see Fig. 5. From the long time exposure photography reported by Cheng et al. [18], the lift-off height can be estimated to be  $x/D = 25$  thanks to the position of the sharp rise in visible light intensity. The computed mean temperature field reported in Fig. 5 is in fairly good qualitative agreement with this estimate. This is confirmed by a more quantitative inspection of computational results versus experimental data: Fig. 5 compares the mean temperature profiles as obtained from the numerical simulations with experimental data at four distinct locations downstream of the injector exit. From the experimental point of view, at the first position  $x/D = 0.85$  close to the injectors, no reaction is observed. Further downstream, at  $x/D = 21.5$  and  $x/D = 32.3$ , the chemical reaction completes and the turbulent diffusion flame stabilizes. The profile obtained at  $x/D = 43$  shows that the length of the diffusion flame is a little bit underestimated with respect to the experimental investigations. This can be explained as follows. As suggested in the studies of Cheng et al. [18], the experimental data obtained at  $x/D = 0.85$  have been used as boundary condition inputs for the CFD simulations and the velocity decrease is thus overestimated. The resulting difference in terms of axial velocity at  $x/D = 0.85$  can reach about 15% which is sufficient to explain the observed difference between numerical simulations and experimental results.

Finally, supersonic combustion in a non-premixed coflowing jet geometry has been successfully computed and the turbulent non-premixed flames obtained with the present approach are in good agreement with the experimental data. The quality of the prediction in terms of both the lift-off height and mean temperature profiles compares well with experimental data. The results are also similar to those obtained in previous studies based on either assumed multivariate

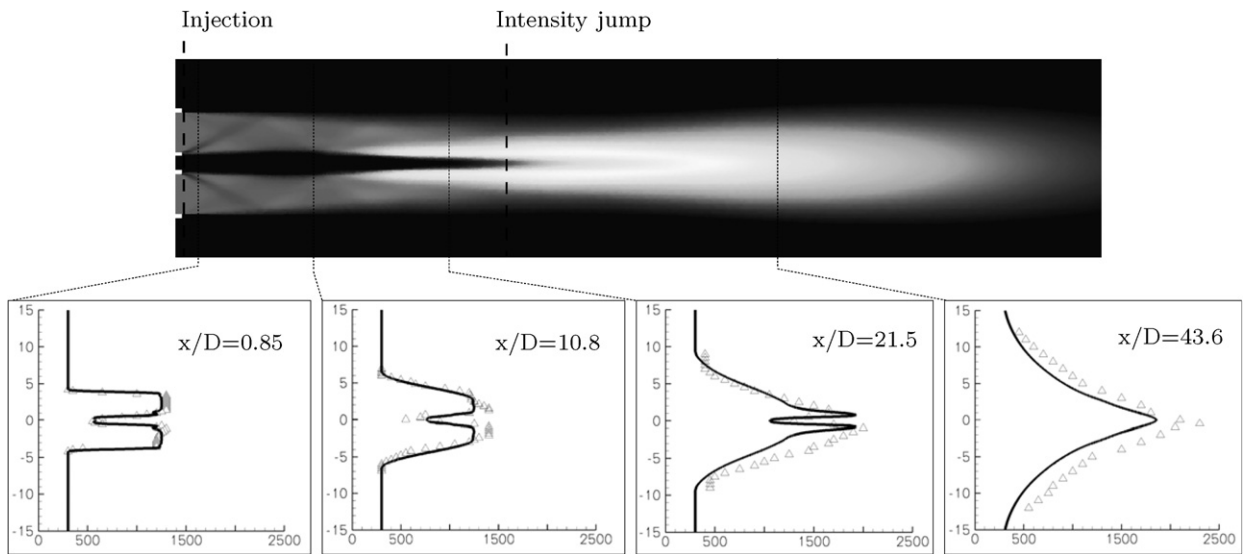


Fig. 5. Supersonic non-premixed lifted flame: comparisons between temperature profiles from experiments (line) and from numerical simulation (symbols).

PDF, see [19], or on joint scalar-velocity-frequency Monte Carlo PDF simulations [20]. This has been confirmed by a more complete survey about the comparison with this experimental database [11] together with the application of the model to a second test case [13]. After this preliminary validation step applied to a well-documented supersonic coflowing jet database, the next section aims at reporting recent results obtained with the same computational strategy, but applied to underexpanded supersonic turbulent reactive flows that are representative of the GH2/GO2 torch igniter used to initiate combustion in a cycle expander engine.

## 5. Underexpanded supersonic coflowing reactive jets

A direct application of the computational model described in the previous section consists in simulating the non-premixed turbulent diffusion flame that arises in the highly underexpanded GH2/GO2 torch jet used to ignite the engine. The rocket engine is composed of several peripheral rings of cryogenic LOX/GH2 injectors, and its full simulation, including all the physical phenomena i.e. underexpanded compressible turbulent and reactive flow with supercritical conditions, still remains challenging. In a first step of the analysis, attention is focused on the simulation of the central underexpanded GH2/GO2 torch jet igniter. The corresponding geometry presents several specific difficulties arising, among others, from the birth of a Mach disk featuring triple point conditions. Favorable conditions for flame stabilization are expected to be found in the high velocity shear layer that establishes between the central jet and the coflowing jet of hydrogen. A satisfactory description of this geometry is then a prerequisite to capture the subsequent interaction of the central torch with the peripheral injectors.

### 5.1. Description of the torch igniter

The igniter is located at the centre of the circular injection plate and it is made of two coflowing streams: a central main jet of vitiated oxygen surrounded by an annular coflowing jet of pure gaseous hydrogen. A 2D axisymmetrical simulation of the combustion chamber is then sufficient to describe it. The central jet is fed by the products of a pre-combustion burner fed with gaseous hydrogen and with an excess of oxygen. The resulting hot mixture is sonically ejected through a nozzle into the engine combustion chamber. The coaxial circulation of cold hydrogen is used to cool the pre-combustor burner: in the numerical simulations we consider that the hydrogen is injected into the combustion chamber at its final temperature and velocity.

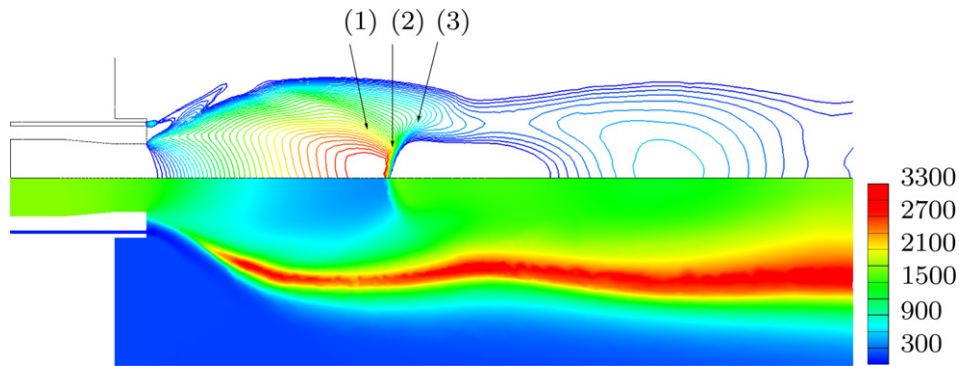


Fig. 6. Mach number isovalues and mean temperature field as obtained from the reactive simulation of the gaseous GH<sub>2</sub>/GO<sub>2</sub> torch jet igniter. 1: Incident shock wave. 2: Mach disk at the triple point separation. 3: Reflected shock wave.

### 5.2. Mesh adaptation strategy

Since the engine is expected to be ignited in space, the pressure levels can be very low in the transient period that precedes the injection of the cryogenic reactants into the combustion chamber and the corresponding pressure ratio gives rise to underexpanded jets. In the absence of any further information about the pressure ratio value, a parametric study has been conducted and several pressure ratios have been considered. Attention is focused below on a single intermediate value of the NPR = 16. In these conditions, the Mach Disk (MD) directly interacts with the shear layer, giving rise to flow instabilities so that no stationary compressible structure can be a priori identified downstream of the Mach disk. The description of the highly underexpanded jet requires a sufficient level of accuracy especially when both the Mach Disk location and the dimensions of the associated core are concerned. In particular, the representation of the resulting mixing layer is essential to estimate the self-ignition conditions that contributes to the turbulent diffusion flame stabilization. This is one of the main reasons that explains why we resort to the AMA strategy in order to increase the precision of the final solution.

The anisotropic mesh adaptation strategy of Dolejsi [16] already described in Section 3 is used here. The choice of the density as an indicator field to apply the remeshing technique does not only lead to a mesh refinement at the discontinuity locations but also improves the description of the mixing layer between hydrogen and oxygen that exhibits a significant density ratio namely  $\rho_{air}/\rho_{H_2} \approx 10$ . The structure of the peculiar flow under consideration is significantly influenced by the coflowing stream of hydrogen. Indeed, the dimensions of the classical single stream underexpanded jet can be rather well estimated by resorting to empirical correlations that allow one to estimate the Mach disk position on the symmetry axis as a function of the Nozzle Pressure Ratio. Such an empirical correlation has been proposed for instance by Ashkenas and Sherman [21]:  $X_{DM}/D_e = 0.67 \times \sqrt{P_e/P_a}$ . Discrepancies of the order of 10 or 15% can usually be found between the results of numerical simulations and the use of such a correlation that has been established from Schlieren imaging (i.e. by means of a time averaging procedure applied along the optical path in the direction of observation) can be discussed in terms of both its applicability and accuracy. It is noteworthy that, in the present case, the results of the numerical simulation show a Mach disk positioned around 30 mm, which is two times larger than the value predicted by using the correlation of Ashkenas and Sherman [21]. The influence of the surrounding jet of hydrogen then deserves to be more deeply studied and the reported results evidence that the underexpanded jet structure is significantly influenced by both the coflowing stream of hydrogen and the turbulent diffusion flame, see Fig. 6.

### 5.3. Stabilization of the turbulent diffusion flame

Fig. 7 displays four consecutive snapshots of the mean temperature field corresponding to the chronology of the stabilization of the turbulent diffusion flame. The first steps of the transient numerical simulation show that the reactive mixture first ignites in the shear layer between the two coflowing streams. Then, the simultaneous decay of turbulent mixing intensity and the presence of hot burned gases make possible the stabilization of a turbulent non-premixed flame in the mixing layer, see Fig. 6.

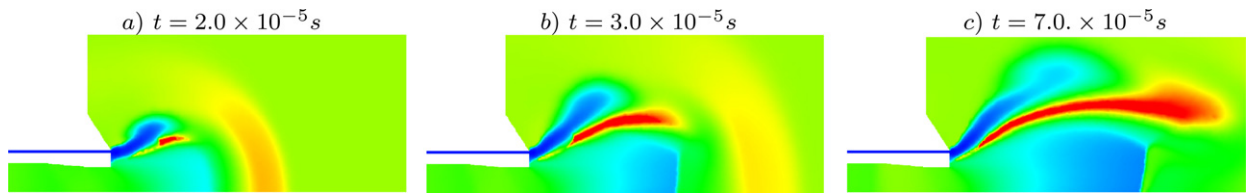


Fig. 7. Fields of the mean temperature at different times during the transient numerical simulation.

## 6. Conclusions and perspectives

A Lagrangian model of turbulent combustion in high speed flows has been used in conjunction with an efficient RANS–AMA strategy to simulate both non-reactive and reactive turbulent supersonic coflowing jets. The Lagrangian model of turbulent combustion relies on the original proposal of Borghi and coworkers which has been extended to address the high Mach number ignition phenomena associated to the conversion of kinetic energy into thermal energy via the viscous dissipation heating. The model is applied to academic test cases as well as to highly underexpanded coflowing jets that gather the essential features of the torch igniter. The obtained results are in satisfactory agreement with both underlying physics and experimental data when available. The forthcoming steps of the present work will concern the interaction of the torch igniter with a peripheral LO<sub>x</sub>/GH<sub>2</sub> injection. The corresponding gaseous study will be completed by performing two-phase flows simulations in the forthcoming months.

## Acknowledgements

Financial support from CNES and SNECMA (SAFRAN Group, Space Engines Division) and from CNRS is gratefully acknowledged.

## References

- [1] V. Morgenthaler, L.F. Figueira da Silva, B. Deshaies, V.A. Sabel'nikov, Non-premixed combustion in supersonic turbulent flows: a numerical study for co-flowing H<sub>2</sub>–air jets, AIAA Paper 99-4917, 1999.
- [2] U. Wepler, W.W. Koschel, Numerical investigation of turbulent reacting flows in a scramjet combustor model, AIAA paper 2002-3572, 2002.
- [3] V.A. Sabel'nikov, B. Deshaies, L.F. Figueira da Silva, Revisited flamelet model for non premixed combustion in supersonic turbulent flows, Combustion and Flame 114 (1998) 577–584.
- [4] M. Obounou, M. Gonzalez, R. Borghi, A Lagrangian model for predicting turbulent diffusion flames with chemical kinetic effects, Proceedings of the Combustion Institute 25 (1994) 1107–1113.
- [5] W.H. Press, B.P. Flannery, S.A. Teukolsky, W.T. Vetterling, Numerical Recipes in Fortran 90. The Art of Parallel Scientific Computing, Cambridge University Press, 1999.
- [6] J. Villermaux, J.C. Devillon, Représentation de la coalescence et de la redispersion des domaines de ségrégation dans un fluide par un modèle d'interaction phénoménologique, in: Proceedings of the 2nd International Symposium on Chemical Reaction Engineering, Amsterdam, vol. B, Elsevier, 1972, pp. 1–13.
- [7] A. Mura, F.X. Demoulin, Lagrangian intermittent modeling of turbulent lifted flames, Combustion Theory and Modelling 11 (2) (2007) 227–257.
- [8] A. Mura, R. Borghi, Towards an extended scalar dissipation equation for turbulent premixed combustion, Combustion and Flame 133 (2003) 193–196.
- [9] A. Mura, K. Tsuboi, T. Hasegawa, Modelling of the correlation between velocity and reactive scalar gradients in turbulent flames based on DNS data, Combustion Theory and Modelling 12 (4) (2008) 671–698.
- [10] C.J. Jachimowski, An analytical study of the hydrogen–air reaction mechanism with application to scramjet combustion, NASA Technical Paper 2791, 1988.
- [11] J.F. Izard, G. Lehnasch, A. Mura, A Lagrangian model of combustion in high speed flows: application to scramjet conditions, Combustion Science and Technology, submitted for publication.
- [12] K.H. Luo, K.N.C. Bray, Combustion-induced pressure effects in supersonic diffusion flames, Proceedings of the Combustion Institute 27 (1998) 2165–2171.
- [13] J.F. Izard, A. Mura, A Lagrangian model for non-premixed combustion in supersonic turbulent flows, in: Proceedings of the 18th International Shock Interaction Symposium, Rouen (France), 15–18 July 2008, pp. 207–212.
- [14] O. Zeman, Dilatation dissipation: the concept and application in modeling compressible mixing layers, Physics of Fluids 2 (2) (1990) 176–188.
- [15] R. Martin, Projet N3SNatur, Version 1.4, Manuel Théorique, Simulog FRANCE, 2001.
- [16] V. Dolejsi, Anisotropic mesh adaptation technique for viscous flow simulation, East–West Journal of Numerical Mathematics 9 (1) (2001) 1–24.

- [17] G. Lehnasch, P. Bruel, A robust methodology for RANS simulations of highly underexpanded jets, *International Journal for Numerical Methods in Fluids* 56 (12) (2008) 2179–2205.
- [18] T.S. Cheng, J.A. Wehrmeyer, R.W. Pitz, O. Jarret, G.B. Northam, Raman measurement of mixing and finite-rate chemistry in a supersonic hydrogen–air diffusion flame, *Combustion and Flame* 99 (1994) 157–173.
- [19] R.A. Baurle, S.S. Girimaji, Assumed turbulence-chemistry closure with temperature–composition correlation, *Combustion and Flame* 134 (2003) 131–148.
- [20] H. Möbus, P. Gerlinger, D. Brüggemann, Scalar and joint scalar-velocity-frequency Monte Carlo PDF simulation of supersonic combustion, *Combustion and Flame* 132 (1–2) (2003) 3–24.
- [21] H. Ashkenas, F.S. Sherman, The structure and utilization of supersonic free jets in low density wind tunnel, in: *Advances in Applied Mathematics – Rarefied Gas Dynamics*, Academic, New York, 1966, pp. 84–105.